A Fully Relativistic Approach to Photon Scattering and Photoionization of Alkali Atoms

Adam Singor [1,*] , **Dmitry Fursa** [1] , **Igor Bray** [1] **and Robert McEachran** [2]

[1] Department of Physics and Astronomy, Curtin University, Perth 6102, Australia; d.fursa@curtin.edu.au (D.F.); igor.bray@curtin.edu.au (I.B.)
[2] Laser Physics Centre, RSP, Australian National University, Canberra 0200, Australia; robert.mceachran@anu.edu.au
[*] Correspondence: adam.singor@postgrad.curtin.edu.au

Abstract: A fully relativistic approach to calculating photoionization and photon-atom scattering cross sections for quasi one-electron atoms is presented. An extensive set of photoionization cross sections have been calculated for alkali atoms: lithium, sodium, potassium, rubidium and cesium. The importance of relativistic effects and core polarization on the depth and position of the Cooper minimum in the photoionization cross section is investigated. Good agreement was found with previous Dirac-based *B*-spline *R*-matrix calculations of Zatsarinny and Tayal and recent experimental results.

Keywords: rayleigh; raman; photon scattering; alkali; photoionization

1. Introduction

A fully quantum mechanical approach to photon-atom scattering processes has been well understood since the mid 1920s with the development of the Kramers–Heisenberg–Waller (KHW) matrix elements [1,2]. The KHW matrix elements describe photon–atom interactions to second order in perturbation theory. Since then, photon–atom and photon–molecule scattering cross sections have proved to be essential for many applications, such as modelling opacity and radiative transport [3–5], Raman spectroscopy [6], and quantum illumination and radar [7,8].

The photoionization of alkali metal atoms has been of particular interest due to the Cooper minimum that occurs in their cross sections near the ionization threshold. Seaton [9] used Hartree–Fock wavefunctions to perform a thorough investigation of the photoionization of the ground state of sodium and discussed the finite minimum observed in the photoionization cross sections for sodium, potassium, rubidium, and cesium. Seaton proposed that the spin–orbit perturbation of continuum wavefunctions would lead to the calculation of a non-zero minimum in the cross section at an incident photon energy between the incident photon energies for which the $\langle ns_{1/2}|D|\epsilon p_{1/2}\rangle$ and $\langle ns_{1/2}|D|\epsilon p_{3/2}\rangle$ dipole matrix elements vanish; this is in agreement with anomalies observed by Fermi [10]. Cooper [11] investigated the photoionization of multiple atoms and ions, including sodium, and demonstrated that the shape of the photoionization cross sections can be understood by considering the energy dependence of the dipole matrix elements. Cooper noted that the minimum in the ground state photoionization cross section of sodium was due the to the cancelation of positive and negative contributions from the radial integral in the calculation of dipole matrix elements.

Early experiments [12–15] measured cross sections that contained contributions from both atomic and molecular photoionization. Accurate vapour pressure data for the target alkali metal was required to calculate separate atomic and molecular cross sections. In general, there was poor agreement between experiments and available theoretical results at the time. It was proposed that this disagreement is likely due to an incorrect or incomplete account of the molecular contribution to the photoionization cross section. Sandner et al. [16]

experimentally measured the ground state photoionization cross section of potassium using a time-of-flight technique that entirely avoids the problem of molecular photoionization that was present in earlier experiments. Since the experiment of Sandner et al. [16], there have been various experiments that have measured photoionization cross sections for the ground and excited states of the alkali atoms [17–22]. The agreement between different experiments has improved in recent times. However, agreement with theory is inconsistent, being poor in many cases.

There have been extensive theoretical investigations into the importance of accounting for core polarization and relativistic effects in regard to obtaining a Cooper minimum at the correct energy and with the correct depth [23–30]. Practically all theoretical calculations have been carried out within a non-relativistic or semi-relativistic formalism, with most calculations utilizing a model potential. The only set of photoionization cross sections produced using a fully relativistic method and accurate atomic structure are those of Zatsarinny and Tayal [30] for potassium. Zatsarinny and Tayal [30] used a Dirac-based *B*-spline *R*-matrix method to calculate the photoionization cross section of the 4*s* ground state and 5*s*–7*s*, 4*p*, 3*d*–5*d* excited states of atomic potassium. They found quadrupole core polarization to be important and obtained excellent agreement with experiment for the 4*s* photoionization cross section, including in the region of the Cooper minimum. The results of Zatsarinny and Tayal [30] are in excellent agreement with more recent experiments [16,20–22] but are generally in poor agreement with previous calculations. The purpose of this paper is to investigate the origin of the differences between the results of Zatsarinny and Tayal and previous theoretical calculations. In particular, we would like to investigate if a model potential approach that can easily be applied to quasi one-electron atoms can produce cross sections of a similar accuracy to the much more complicated and computationally expensive *R*-matrix approach if relativistic effects and core polarization are adequately accounted for.

Recently, we have developed two computational methods for calculating photoionization, Rayleigh and Raman scattering cross sections for hydrogen-like atoms that are valid for incident photon energies above and below the ionization threshold [31,32]. The first method involves the direct numerical calculation of KHW matrix elements and utilizes principal value integration to deal with pole terms. The second method implements a finite-L^2 expansion of the target and deals with pole terms by using a complex scaling technique that has been widely used to study resonances in atoms and molecules [33–35]. Here, the first of these techniques is extended to a fully relativistic formalism for quasi one-electron atoms and applied to the calculation of photoionization, Rayleigh and Raman scattering cross sections for alkali atoms: lithium, sodium, potassium, rubidium, and cesium. In the next section, we give a brief formulation of photon scattering based on the Dirac equation. In Section 3, we present the the target structure model for the alkali atoms and the computational technique. In Section 4, the importance of accounting for core polarization is demonstrated, the significance of relativistic effects is investigated, the sensitivity of the depth and location of the Cooper minimum to changes in the structure model are explored, and an extensive set of photoionization cross sections for the alkali atoms are presented and compared with available previous calculations. Conclusions and future directions are formulated in Section 5. We use atomic units in this paper, unless stated otherwise.

2. Theory

The detailed formalism we recently developed for photoionization, Rayleigh and Raman scattering on quasi one-electron atoms is discussed in [31,32]. Here, we present the details of its extension to the fully relativistic formalism. This formalism allows for the efficient calculation of Rayleigh and Raman scattering cross sections; however, it can also produce photoionization cross sections with very little additional computation.

The differential cross section for Rayleigh or Raman scattering from an initial state $|i\rangle$ to a final state $|f\rangle$ in the length gauge is

$$\frac{\mathrm{d}\sigma_{fi}}{\mathrm{d}\Omega} = r_0^2 \omega \omega'^3 \left| M_{fi} \right|^2. \tag{1}$$

Here, the KHW matrix elements in the length gauge are

$$M_{fi} = \sum_t \left[\frac{\langle f | \boldsymbol{r} \cdot \hat{\boldsymbol{\epsilon}}'^* | t \rangle \langle t | \boldsymbol{r} \cdot \hat{\boldsymbol{\epsilon}} | i \rangle}{E_t - E_i - \omega - \mathrm{i}0} + \frac{\langle f | \boldsymbol{r} \cdot \hat{\boldsymbol{\epsilon}} | t \rangle \langle t | \boldsymbol{r} \cdot \hat{\boldsymbol{\epsilon}}'^* | i \rangle}{E_t - E_i + \omega'} \right], \tag{2}$$

where E_t is the relativistic energy of the state $|t\rangle$, ω (ω') and $\hat{\boldsymbol{\epsilon}}$ ($\hat{\boldsymbol{\epsilon}}'$) are the incident (scattered) photon energy and polarization, respectively [36]. The integrated Rayleigh or Raman cross section for scattering of unpolarized light from an initial state $|i\rangle$ to a final state $|f\rangle$ is given by [32]

$$\sigma_{fi} = \sigma_{\mathrm{T}} \frac{\omega \omega'^3}{3(2j_i + 1)} \sum_{\mu=0}^{2} (2\mu + 1) \left| A_{fi}^{(\mu)} \right|^2, \tag{3}$$

where $\sigma_{\mathrm{T}} = 8\pi r_0^2/3 \approx 6.652 \times 10^{-29}$ m^2 is the Thomson cross section. The tensor expansion coefficients are

$$A_{fi}^{(\mu)} = (-1)^{j_i + j_f + \mu} \sum_t \begin{Bmatrix} j_i & j_f & \mu \\ 1 & 1 & j_t \end{Bmatrix} \langle n_f \kappa_f || D || n_t \kappa_t \rangle \langle n_t \kappa_t || D || n_i \kappa_i \rangle$$

$$\times \left[\frac{1}{E_t - E_i - \omega - \mathrm{i}0} + \frac{(-1)^{\mu}}{E_t - E_i + \omega'} \right], \tag{4}$$

and the relativistic reduced electric dipole matrix elements in the Babushkin gauge are [37–39]

$$\langle n'\kappa' || D || n\kappa \rangle = (-1)^{\kappa'} \sqrt{(2j+1)(2j'+1)} \begin{pmatrix} j' & 1 & j \\ \tfrac{1}{2} & 0 & -\tfrac{1}{2} \end{pmatrix} \Pi(\kappa', \kappa, 1)$$

$$\times \frac{3c}{2\mathcal{E}} \left\{ 2J^{(1)}(\mathcal{E}) + [(\kappa - \kappa') I_2^+(\mathcal{E}) + 2I_2^-(\mathcal{E})] \right\}. \tag{5}$$

Here,

$$\Pi(\kappa', \kappa, \lambda) = \frac{1}{2} \left(1 - \frac{\kappa}{|\kappa|} \frac{\kappa'}{|\kappa'|} (-1)^{j+j'+\lambda} \right), \tag{6}$$

$$I_\lambda^+(\mathcal{E}) = \int_0^\infty \mathrm{d}r \left(u_{n\kappa}^{\mathrm{L}}(r) u_{n'\kappa'}^{\mathrm{S}}(r) + u_{n\kappa}^{\mathrm{S}}(r) u_{n'\kappa'}^{\mathrm{L}}(r) \right) j_\lambda \left(\frac{\mathcal{E}r}{c} \right), \tag{7}$$

$$I_\lambda^-(\mathcal{E}) = \int_0^\infty \mathrm{d}r \left(u_{n\kappa}^{\mathrm{L}}(r) u_{n'\kappa'}^{\mathrm{S}}(r) - u_{n\kappa}^{\mathrm{S}}(r) u_{n'\kappa'}^{\mathrm{L}}(r) \right) j_\lambda \left(\frac{\mathcal{E}r}{c} \right), \tag{8}$$

$$J^{(\lambda)}(\mathcal{E}) = \int_0^\infty \mathrm{d}r \left(u_{n\kappa}^{\mathrm{L}}(r) u_{n'\kappa'}^{\mathrm{L}}(r) + u_{n\kappa}^{\mathrm{S}}(r) u_{n'\kappa'}^{\mathrm{S}}(r) \right) j_\lambda \left(\frac{\mathcal{E}r}{c} \right), \tag{9}$$

where $\Pi(\kappa', \kappa, \lambda)$ accounts for the parity selection rule that $\ell' + \lambda + \ell$ must be even, $u_{n\kappa}^{\mathrm{L}}(r)$ and $u_{n\kappa}^{\mathrm{S}}(r)$ are the large and small components of the radial wavefunction, respectively, and $\mathcal{E} = |E' - E|$ and $j_\lambda(x)$ are spherical Bessel functions of the first kind. In the non-relativistic limit, (5) reduces to the usual length gauge dipole matrix element. We make the Pauli approximation for the calculation of the length gauge dipole matrix elements

$$\langle n'\kappa'||D||n\kappa\rangle = \langle n'\kappa'||r||n\kappa\rangle \tag{10}$$

$$= (-1)^{\kappa'}\sqrt{(2j+1)(2j'+1)}\begin{pmatrix} j' & 1 & j \\ \frac{1}{2} & 0 & -\frac{1}{2} \end{pmatrix}\Pi(\kappa',\kappa,1)$$

$$\times \int_0^\infty dr\left[u_{n'\kappa'}^{\mathrm{L}}(r)\,r\,u_{n\kappa}^{\mathrm{L}}(r) + u_{n'\kappa'}^{\mathrm{S}}(r)\,r\,u_{n\kappa}^{\mathrm{S}}(r)\right], \tag{11}$$

which is practically identical to the fully relativistic form for the neutral alkali atoms we consider here. This form also allows core polarization to be accounted for in a straightforward way, which will be discussed in Section 3.1.

The cross section for photoionization from some state $|i\rangle$ by a photon with polarization $\hat{\boldsymbol{\epsilon}}$ and energy ω is

$$\sigma_i^{\mathrm{ion}} = \sigma_T \frac{3\pi}{2}c^3\omega \sum_t |\langle n_i\kappa_i m_i|\hat{\boldsymbol{\epsilon}}\cdot\boldsymbol{r}|(E_i+\omega)\kappa_t m_t\rangle|^2, \tag{12}$$

which can be rewritten as [40]

$$\sigma_i^{\mathrm{ion}} = \sigma_T \frac{3\pi}{2}\frac{c^3\omega}{3(2j+1)}\sum_t |\langle n_i\kappa_i||r||(E_i+\omega)\kappa_t\rangle|^2. \tag{13}$$

Within our formalism, the photoionization cross section can be obtained using

$$\sigma_i^{\mathrm{ion}} = \sigma_T \frac{3}{2}\frac{c^3\omega}{\sqrt{3(2j+1)}}\,\mathrm{Im}\left\{A_{ii}^{(0)*}\right\}. \tag{14}$$

If individual fine structure cross sections are not of interest, then combined cross sections can be found by averaging over the initial total angular momentum and summing over the final total angular momentum,

$$\sigma_{n_f\ell_f n_i\ell_i} = \sum_{j_i j_f}\frac{(2j_i+1)}{(2s_i+1)(2\ell_i+1)}\sigma_{n_f\ell_f j_f n_i\ell_i j_i}. \tag{15}$$

Equation (15) is valid for Rayleigh, Raman and photoionization cross sections; in the case of Rayleigh scattering and photoionization, the summation is over j_i only.

3. Computational Methods

3.1. Quasi One-Electron Atomic Structure

We modelled the alkali metal atoms as a single electron in a central local potential produced by frozen core electrons. The κ-dependent potential can be written in the following form:

$$V^{(\kappa)}(r) = V_{\mathrm{d}}(r) + V_{\mathrm{e}}^{(\kappa)}(r) + V_{\mathrm{p}}^{(\kappa)}(r). \tag{16}$$

Here, the direct term is

$$V_{\mathrm{d}}(r) = -\frac{Z}{r} + \sum_{n_c\kappa_c}(2\ell_c+1)\int_0^\infty dr'\,\frac{|\phi_{n_c\kappa_c}(r')|^2}{\max(r,r')}, \tag{17}$$

where the $\phi_{n_c\kappa_c}(r)$ are core orbitals obtained from GRASP [41]. We used the equivalent local exchange term introduced by Furness and McCarthy [42]

$$V_{\mathrm{e}}^{(\kappa)}(r) = -\frac{\alpha_{\mathrm{exch}}^{(\kappa)}}{2}\left\{\left[(E-V_{\mathrm{d}}(r))^2 + 4\pi\rho(r)\right]^{1/2} - (E-V_{\mathrm{d}}(r))\right\}, \tag{18}$$

where

$$\rho(r) = \sum_{n_c \kappa_c} (2\ell_c + 1) \frac{\phi_{n_c \kappa_c}^2(r)}{4\pi r^2} \tag{19}$$

is the electron density of the core and $\alpha_{\text{exch}}^{(\kappa)}$ is a parameter that is chosen, for each relativistic quantum number κ, to ensure the local exchange potential is equivalent to its non-local counterpart. The local exchange approximation and the exact non-local exchange potentials are equivalent in the sense that they both produce the same spectrum. We set $E = 0$ to ensure orthogonal orbitals [43]. The dipole polarization potential is given by [25]

$$V_{\text{P}}^{(\kappa)}(r) = -\frac{\alpha_{\text{D}}}{2r^4} \left\{ 1 - \exp\left[-\left(\frac{r}{r_c^{(\kappa)}} \right)^6 \right] \right\}, \tag{20}$$

where α_{D} is the static dipole polarizability of the core ion, $r_c^{(\kappa)}$ is a cut-off radius chosen to reproduce the lowest experimental energy level above the core for each κ.

To account for dipole core polarization more accurately, we have also preformed calculations using the modified length form of the dipole operator [44,45]

$$r \rightarrow r - \frac{\alpha_{\text{D}}}{r^2} \left\{ 1 - \exp\left[-\left(\frac{r}{\tilde{r}_c} \right)^6 \right] \right\}^{1/2}, \tag{21}$$

where α_{D} is the static dipole polarizability of the core ion and the cut-off radius $\tilde{r}_c$ is chosen to reproduce the weighted average of the experimental resonant transition oscillator strengths. If both dipole and quadrupole core polarization are required, as is suggested by Zatsarinny and Tayal [30] for the $4p$ states of potassium, then the following modified dipole operator is used [46]

$$r \rightarrow r - \frac{\alpha_{\text{D}}}{r^2} \left\{ 1 - \exp\left[-\left(\frac{r}{\tilde{r}_c'} \right)^3 \right] \right\} - \frac{\alpha_{\text{Q}}}{r^4} \left\{ 1 - \exp\left[-\left(\frac{r}{\tilde{r}_c'} \right)^5 \right] \right\}, \tag{22}$$

where α_{Q} is the static quadrupole polarizability of the core ion and the cut-off radius is chosen in the same way as before.

We also used dipole and quadrupole polarization potentials produced using the polarized orbital method of McEachran et al. [47]. These polarization potentials were rescaled for each κ to reproduce experimental energy levels. This rescaling was carried out at intermediate radial distances to ensure the asymptotic form of the potential remain unchanged. We found that, after fitting to experimental energy levels, both potentials produce practically identical spectra and lead to practically the same cross sections. These polarization potentials can also be used in the construction of the modified dipole operator. A cut-off function can be obtained by multiplying a polarization potential by the reciprocal of its asymptotic form and then taking the square root. These cut-off functions replace the cut-off functions in (22). Similarly, these cut-off functions are rescaled at an intermediate radial distance to reproduce the weighted average of the experimental resonant transition oscillator strengths. After fitting to resonant transition oscillator strengths, we found that calculations performed using the three different forms of the modified dipole operator—two analytic, (21) and (22), and one numerical—produce cross sections that are practically indistinguishable. In what follows, we will use only the modified dipole operator given by (21) with parameters given in Table 1.

The parameters used to construct the central local potentials for each atom are given in Table 1. We chose to use a κ-dependent potential as it yields more accurate energy levels, though it leads to a small discrepancy between cross sections calculated using the length and velocity forms of the dipole operator.

Table 1. Local central model potential parameters for alkali atoms. The "−" indicates that this part of the potential is found to be insignificant. The static dipole and quadrupole polarizability of the core ions are from [48,49].

Parameter	Lithium	Sodium	Potassium	Rubidium	Cesium
α_D	0.194	1.001	5.515	9.143	15.805
α_Q	0.0047	0.0634	0.733	1.592	4.907
$\alpha_{\text{exch}}^{(-1)}$	1.130	0.987	1.161	1.140	1.212
$\alpha_{\text{exch}}^{(1)}$	0.769	1.068	1.220	1.203	1.257
$\alpha_{\text{exch}}^{(-2)}$	0.769	1.069	1.224	1.120	1.298
$\alpha_{\text{exch}}^{(2)}$	0.392	0.714	1.022	1.111	1.202
$\alpha_{\text{exch}}^{(-3)}$	0.392	0.724	1.026	1.126	1.233
$\alpha_{\text{exch}}^{(3)}$	5.001	1.251	0.626	0.626	0.724
$\alpha_{\text{exch}}^{(-4)}$	5.001	1.251	0.626	0.626	0.763
$r_c^{(-1)}$	1.405	1.529	2.259	2.595	2.968
$r_c^{(1)}$	1.292	1.693	2.208	2.561	2.882
$r_c^{(-2)}$	1.291	1.683	2.202	2.559	2.901
$r_c^{(2)}$	2.345	1.798	2.464	2.941	3.325
$r_c^{(-3)}$	2.345	1.817	2.469	2.966	3.386
$r_c^{(3)}$	−	4.376	3.126	3.126	3.009
$r_c^{(-4)}$	−	4.376	3.126	3.126	3.067
$\tilde{r}_c$	3.135	2.834	3.297	3.953	4.398

The qausi one-electron Dirac equation for the active electron is

$$H\psi_{n\kappa m}(\boldsymbol{r}) = \left(c\,\tilde{\boldsymbol{\alpha}} \cdot \boldsymbol{p} + \tilde{\beta}c^2 + V^{(\kappa)}(r)\right)\psi_{n\kappa m}(\boldsymbol{r}) = E\,\psi_{n\kappa m}(\boldsymbol{r}), \tag{23}$$

where $\tilde{\boldsymbol{\alpha}}$ and $\tilde{\beta}$ are the Dirac matrices, $\boldsymbol{p}$ is the momentum operator, and c is the speed of light. Atomic target states can be expanded in terms of Dirac L-spinors which are the relativistic analogue of the Coulomb Sturmian functions. The relativistic wavefunction can be expanded as [50]

$$\psi_{n\kappa m}(\boldsymbol{r}) = \frac{1}{r}\begin{pmatrix} \psi_{n\kappa}^L(r)\,\chi_{\kappa m} \\ i\psi_{n\kappa}^S(r)\,\chi_{-\kappa m} \end{pmatrix} = \frac{1}{r}\begin{pmatrix} \sum_{n_r} c_{nn_r}^L f_{n_r\kappa}^L(r)\,\chi_{\kappa m} \\ i\sum_{n_r} c_{nn_r}^S f_{n_r\kappa}^S(r)\,\chi_{-\kappa m} \end{pmatrix}, \tag{24}$$

where $f_{n_r\kappa}^L(r)$ and $f_{n_r\kappa}^S(r)$ are Dirac L-spinors. The explicit form of the Dirac L-spinors is

$$f_{n_r\kappa}^{L/S}(r) = \left[\frac{n_r!\,(2\gamma + n_r)}{2N_{n_r\kappa}(N_{n_r\kappa} - \kappa)\Gamma(2\gamma + n_r)}\right]^{1/2}(2\lambda r)^\gamma e^{-\lambda r}$$
$$\times \left(-(1 - \delta_{n_r 0})L_{n_r-1}^{2\gamma}(2\lambda r) \pm \frac{N_{n_r-\kappa}}{n_r + 2\gamma}L_{n_r}^{2\gamma}(2\lambda r)\right), \tag{25}$$

where $\gamma = \left[\kappa^2 - (Z/c)^2\right]^{1/2}$, $N_{n_r\kappa} = \left[\kappa^2 + 2n_r\gamma + n_r^2\right]^{1/2}$, $\Gamma(z)$ is the usual Gamma function, $L_m^\alpha(x)$ are the associated Laguerre polynomials and the $\pm$ corresponds to the large and small components, respectively. The properties of the Dirac L-spinors are discussed by Grant and Quiney in [50].

The expansion coefficients $\{c_{nn_r}^L, c_{nn_r}^S\}$ and energy eigenvalues $\{E_{n_r}\}$ where $n_r = 1, \ldots, N_\kappa$, are obtained by diagonalizing the Dirac Hamiltonian in a basis of Dirac L-spinors. To do this, we solve a Galerkin equation

$$\begin{bmatrix} mc^2\tilde{s}^{\mathrm{L}} + (\tilde{V}^{(\kappa)})^{\mathrm{L}} & c\tilde{\Pi}^{\mathrm{LS}} \\ c\tilde{\Pi}^{\mathrm{SL}} & -mc^2\tilde{s}^{\mathrm{S}} + (\tilde{V}^{(\kappa)})^{\mathrm{S}} \end{bmatrix} \begin{bmatrix} \tilde{c}^{\mathrm{L}} \\ \tilde{c}^{\mathrm{S}} \end{bmatrix} = E \begin{bmatrix} \tilde{s}^{\mathrm{L}} & \tilde{s}^{\mathrm{S}} \end{bmatrix} \begin{bmatrix} \tilde{c}^{\mathrm{L}} \\ \tilde{c}^{\mathrm{S}} \end{bmatrix}, \tag{26}$$

where the matrix elements are

$$\tilde{s}^{\mathrm{X}}_{n'_r n_r} = \langle f^{\mathrm{X}}_{n'_r \kappa} | f^{\mathrm{X}}_{n_r \kappa} \rangle, \tag{27}$$

$$\tilde{\Pi}^{\mathrm{LS}}_{n'_r n_r} = \langle f^{\mathrm{L}}_{n'_r \kappa} | \frac{\mathrm{d}}{\mathrm{d}r} + \frac{\kappa}{r} | f^{\mathrm{S}}_{n_r \kappa} \rangle \tag{28}$$

$$= - \langle f^{\mathrm{L}}_{n'_r \kappa} | \frac{-N_{n_r \kappa} - n_r - \gamma}{r} + \lambda | f^{\mathrm{L}}_{n_r \kappa} \rangle, \tag{29}$$

$$\tilde{\Pi}^{\mathrm{SL}}_{n'_r n_r} = \langle f^{\mathrm{S}}_{n'_r \kappa} | \frac{\mathrm{d}}{\mathrm{d}r} + \frac{\kappa}{r} | f^{\mathrm{L}}_{n_r \kappa} \rangle \tag{30}$$

$$= - \langle f^{\mathrm{L}}_{n_r \kappa} | \frac{-N_{n'_r \kappa} - n'_r - \gamma}{r} + \lambda | f^{\mathrm{L}}_{n'_r \kappa} \rangle, \tag{31}$$

$$(\tilde{V}^{(\kappa)})^{\mathrm{X}}_{n'_r n_r} = \langle f^{\mathrm{X}}_{n'_r \kappa} | V^{(\kappa)} | f^{\mathrm{X}}_{n_r \kappa} \rangle, \tag{32}$$

and $X = L$ or $X = S$. The diagonalization process results in N_κ states that describe bound states and the discretized continuum as well as another N_κ states representing the discretized negative energy continuum [51]. Bound states for each atom were calculated using this diagonalization approach for each relativistic quantum number κ in a basis of 150 Dirac L-spinors.

Target continuum states satisfying (23) were produced for each required energy $E = c\sqrt{k^2 + c^2}$ by solving a pair of coupled first order differential equations for the large and small components of the radial wavefunction

$$c\left(\frac{\mathrm{d}}{\mathrm{d}r} - \frac{\kappa}{r}\right)\psi^{\mathrm{S}}_{E\kappa}(r) - \left(V^{(\kappa)}(r) - E\right)\psi^{\mathrm{L}}_{E\kappa}(r) = 0, \tag{33a}$$

$$c\left(\frac{\mathrm{d}}{\mathrm{d}r} + \frac{\kappa}{r}\right)\psi^{\mathrm{L}}_{E\kappa}(r) + \left(-2c^2 + V^{(\kappa)}(r) - E\right)\psi^{\mathrm{S}}_{E\kappa}(r) = 0. \tag{33b}$$

These differential equations were solved using an Adams-Moulton predictor–corrector method [52].

3.2. Principal Value Method

Here, we will discuss a fully relativistic implementation of the principal value (PV) method which has previously been used to successfully calculate Rayleigh and Raman scattering on hydrogen and the alkali atoms as well as photoionization from the ground and excited states of hydrogen [31,32]. The relativistic extension of the PV method is virtually identical to the non-relativistic version; thus, we will only discuss the essential elements of the method and any changes from the non-relativistic implementation. The tensor expansion coefficients can be calculated directly by separating the sum in (4) into a sum over bound states and a Cauchy principal value integral over the continuum with an imaginary pole term [53,54]

$$A^{(\mu)}_{n'\kappa'n\kappa} = (-1)^{j+j'+\mu} \sum_t \begin{Bmatrix} j & j' & \mu \\ 1 & 1 & j_t \end{Bmatrix} \left(\sum_{n_t=l_t+1}^{N_b} \langle n'\kappa'||r||n_t\kappa_t\rangle \langle n_t\kappa_t||r||n\kappa\rangle \right.$$

$$\times \left[\frac{1}{E_{n_t\kappa_t} - E_{n\kappa} - \omega} + \frac{(-1)^\mu}{E_{n_t\kappa_t} - E_{n\kappa} + \omega'} \right] + \mathcal{P}\int dE \frac{\langle n'\kappa'||r||E\kappa_t\rangle \langle E\kappa_t||r||n\kappa\rangle}{E - E_{n\kappa} - \omega}$$

$$+ i\pi \langle n'\kappa'||r||(E_{n\kappa} + \omega)\kappa_t\rangle \langle (E_{n\kappa} + \omega)\kappa_t||r||n\kappa\rangle$$

$$\left. + (-1)^\mu \int dE \frac{\langle n'\kappa'||r||E\kappa_t\rangle \langle E\kappa_t||r||n\kappa\rangle}{E - E_{n\kappa} + \omega'} \right). \tag{34}$$

Convergence of the cross sections is achieved by increasing the number of intermediate bound states and quadrature points.

4. Results

In this section, we discuss relativistic effects on Rayleigh, Raman and photoionization cross sections and demonstrate the importance of accounting for core polarization to calculate photoionization cross sections with the Cooper minimum at the correct energy. An extensive set of photoionization cross sections as a function of photoelectron energy is then presented for each alkali atom that includes photoionization from the ground state, the first three excited $s_{1/2}$ states, the first three excited $p_{1/2}$ and $p_{3/2}$ states and the first three $d_{3/2}$ and $d_{5/2}$ excited states. Comparisons to available experimental and theoretical results are made whenever possible. All cross sections are presented in units of the Thomson cross section. Fine structure combined cross sections are presented for photoionization from d states where fine structure splitting was found to be negligible. Cross sections calculated using the PV method will be labelled 'PV-M' if the modified length form of the dipole operator was used and 'PV-L' if the usual length gauge dipole operator was used.

4.1. Rayleigh and Raman Cross Sections

Recently, we calculated Rayleigh and Raman scattering cross sections for the alkali atoms using a semi-relativistic model [32]. Here, we investigate relativistic effects on Rayleigh and Raman scattering cross sections using a fully relativistic model. For the lighter alkali atoms (lithium, sodium, and potassium), we found no difference between our present and previous results. The difference between our present and previous results becomes noticeable for the heavier alkali atoms. We, therefore, use cesium, the heaviest of the considered alkali atoms, to illustrate the situation. In Figure 1, we compare our Rayleigh and Raman cross sections calculated using a fully relativistic approach to those calculated using a non-relativistic formalism that includes a semi-empirical spin–orbit term in the potential and the results presented by Singor et al. [32]. The fully relativistic and non-relativistic sets of cross sections were calculated using the modified length gauge dipole operator (21) with the same cut-off radius to ensure that any difference is due to the relativistic treatment of the atomic structure. In general, relativistic effects lead to a more pronounced splitting of the resonances and a smaller cross section above the ionization threshold; however, these difference are small. The only significant difference between the two sets of cross sections occurs for $6p_{1/2} \rightarrow 4f_{5/2}$ Raman scattering where the relativistic cross section is significantly larger above the ionization threshold. The dipole matrix elements calculated during the construction of this cross section are strongly affected by relativistic effects. Any differences due to relativistic effects are even smaller for the lighter alkali atoms. Comparison with our previous results [32] shows that the choice of the cut-off radius used in the modified operator has a greater influence on the cross section than relativistic effects. Previously, the cut-off radius was taken to be the average of the cut-radii used in the construction of the polarization potential; we have improved upon this by choosing the cut-off radius to reproduce the weighted average of the resonant transition oscillator strengths. This new choice of the cut-off radius accounts

for the difference between our previous and current results. We can conclude that a semi-relativistic model that accounts for spin–orbit interaction and core polarization is sufficient for calculating Rayleigh and Raman scattering cross sections at energies both above and below the ionization threshold.
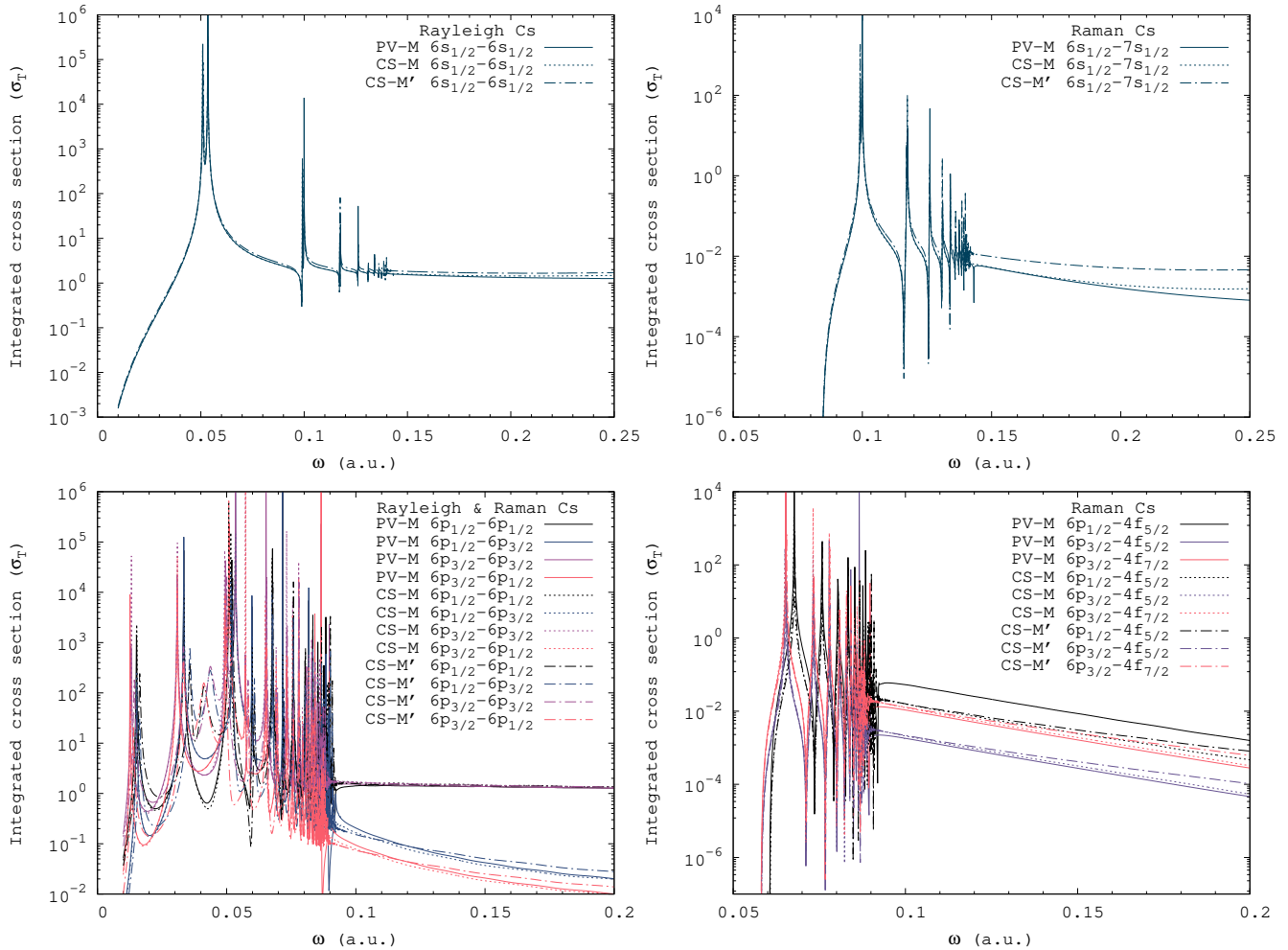

Figure 1. Rayleigh and Raman cross sections for scattering on the ground and first excited p state of cesium calculated using the fully relativistic principal value (PV) method with the modified length form of the dipole operator. We compare with a semi-relativistic (CS-M) calculation and the complex scaling (CS-M') method results of Singor et al. [32], which were calculated using a non-relativistic atomic structure model with a spin–orbit potential and a modified length gauge dipole operator.

4.2. Photoionization Cross Sections

Photoionization cross sections for an s state of an alkali atom, except lithium, have a minimum just above the ionization threshold; this is known as the Cooper minimum [9,11]. In non-relativistic quantum mechanics, this minimum occurs due to the dipole matrix element vanishing, which leads to the minimum in the cross section having a value of zero. In relativistic quantum mechanics, the $\langle ns_{1/2}|D|\epsilon p_{1/2}\rangle$ and $\langle ns_{1/2}|D|\epsilon p_{3/2}\rangle$ dipole matrix elements will vanish at different energies; this leads to a non-zero minimum in the cross section occurring at some energy between where these individual dipole matrix elements vanish. This difference in the depth of the Cooper minimum can be seen in Figure 2 for photoionization from the ground state of rubidium where we compare cross sections calculated using the relativistic and non-relativistic forms of the PV method. However, there is very little difference between the relativistic and non-relativistic cross sections at energies away from the Cooper minimum. We also demonstrate the significant effect

of accounting for core polarization on the position of the Cooper minimum by using the modified dipole operator (21). Cross sections calculated using the standard length gauge dipole operator are compared to those calculated using the modified form in Figure 2. This is carried out in both the relativistic and non-relativistic cases; in the non-relativistic case, we used the same cut-off radius as is used in the fully relativistic case. This ensures that any difference between the non-relativistic and relativistic cross sections is due to relativistic effects only and not some combination of relativistic effects and different cut-off radii for the modified dipole operators. The use of different forms of the modified dipole operator was investigated; it was found that, after fitting the modified dipole operator to reproduce the weighted average of the experimental resonant transition oscillator strengths, that all forms of the operator produce cross sections that are practically identical. Accounting for core polarization through the use of a modified dipole operator leads to the Cooper minimum occurring closer to the ionization threshold. It also leads to a large difference in the magnitude of the cross section at all energies.
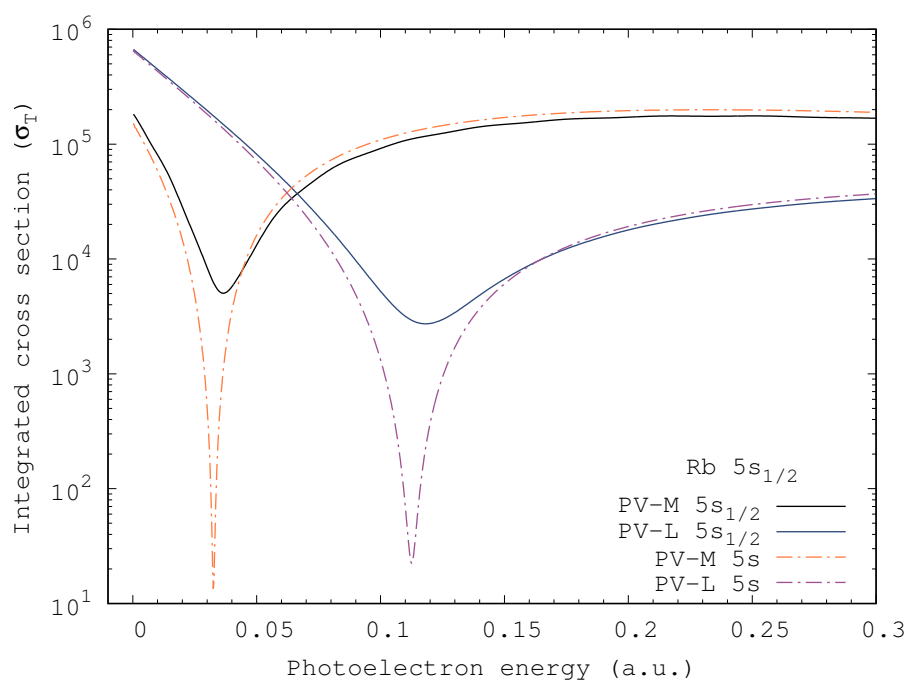

Figure 2. Photoionization cross section for the ground state of rubidium with and without relativistic effects and the modified dipole operator. Non-relativistic calculations were performed using the length gauge dipole operator, a modified dipole operator with the same cut-off radius as the fully relativistic case. The modified dipole operator shifts the Cooper minimum closer to the ionization threshold. Relativistic effects lead to a shallower Cooper minimum.

The photoionization cross sections of Zatsarinny and Tayal [30] are the only other theoretical results calculated in a fully relativistic formalism for the alkali atoms. Their results were produced using a Dirac-based *B*-spline *R*-matrix method which uses the most sophisticated atomic structure model that has been used for single photon ionization of an alkali atom. We therefore chose to validate our results against those of Zatsarinny and Tayal for potassium and propose that our results for the other atoms are of a similar quality. In Figures 3 and 4, we present our results for potassium and compare them with available experimental and theoretical data. We found excellent agreement with the Dirac-based *B*-spline *R*-matrix calculations of Zatsarinny and Tayal [30] for photoionization from *s* and *d* states, but for the $4p_{1/2}$ and $4p_{3/2}$ states, the agreement is not as good. Zatsarinny and Tayal observed that, when calculating binding energies for the $4p$ states, accounting for the dipole polarizability of the core was not sufficient and that higher order polarization was important. We found that including a quadrupole polarization term in the modified dipole operator (22) made practically no difference to our $4p$ cross sections. The cut-off radius

for both the dipole and quadrupole polarization terms in the modified dipole operator was chosen to reproduce the weighted average of the experimental $4s_{1/2} - 4p_{1/2}$ and $4s_{1/2} - 4p_{3/2}$ oscillator strengths. By fitting our polarization potential and modified dipole operator to experimental values, we can effectively account for higher order multipole contributions with just dipole terms, which could explain why including quadrupole terms in our modified dipole operator makes virtually no difference to our cross sections. The polarized pseudostate method employed by Zatsarinny and Tayal results in fixed contributions from each dipole-, quadrupole-, and octopole-polarized pseudostate; thus, they found the inclusion of both dipole- and quadrupole-polarized pseudostates necessary to reproduce experimental $4p$ energy levels of potassium.

The small variance between our $4p$ cross sections and those of Zatsarinny and Tayal is likely due to our use of a simple quasi one-electron structure model in our calculations. The approach used by Zatsarinny and Tayal is not fully ab initio; core polarization is accounted for by using polarized psedostates, which account for single excitation channels from the $3s$ and $3p$ shells. Calculations performed using a target structure model that is more accurate than either ours or Zatsarinny and Tayal's would likely resolve this problem. Our excellent agreement for all other photoionization cross sections reinforces Zatsarinny and Tayal's observation that contributions from core polarization are dominated by dipole polarization for photoionization from s, d, and more highly excited p states.
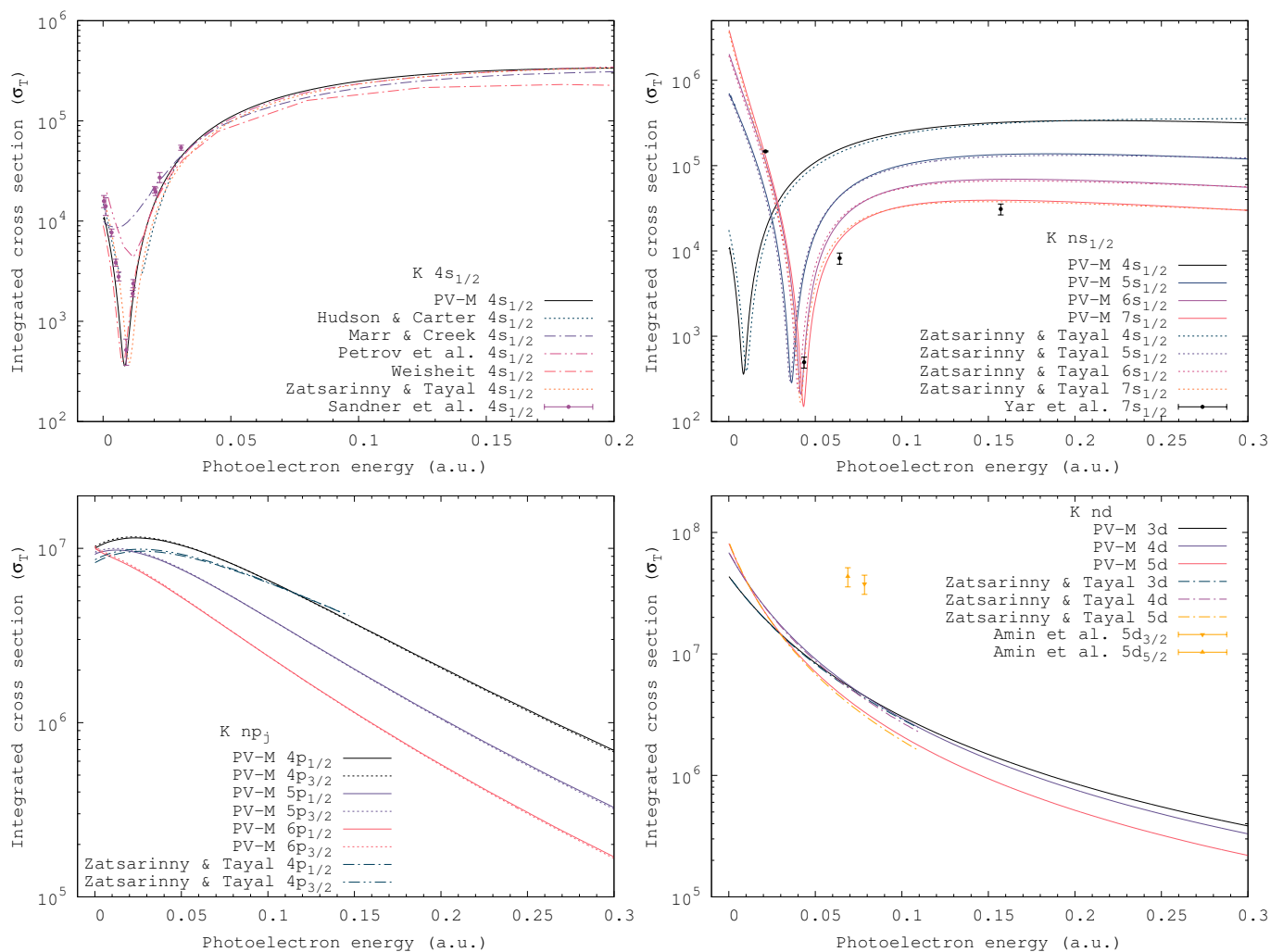

Figure 3. Photoionization cross sections for the ground and excited states of potassium. Our photoionization cross sections are compared with the experimental results of Hudson and Carter [14], Marr and Creek [15], Sandner et al. [16], Yar et al. [21], and Amin et al. [20] and the theoretical calculations of Weisheit [24], Petrov et al. [29], and Zatsarinny and Tayal [30].
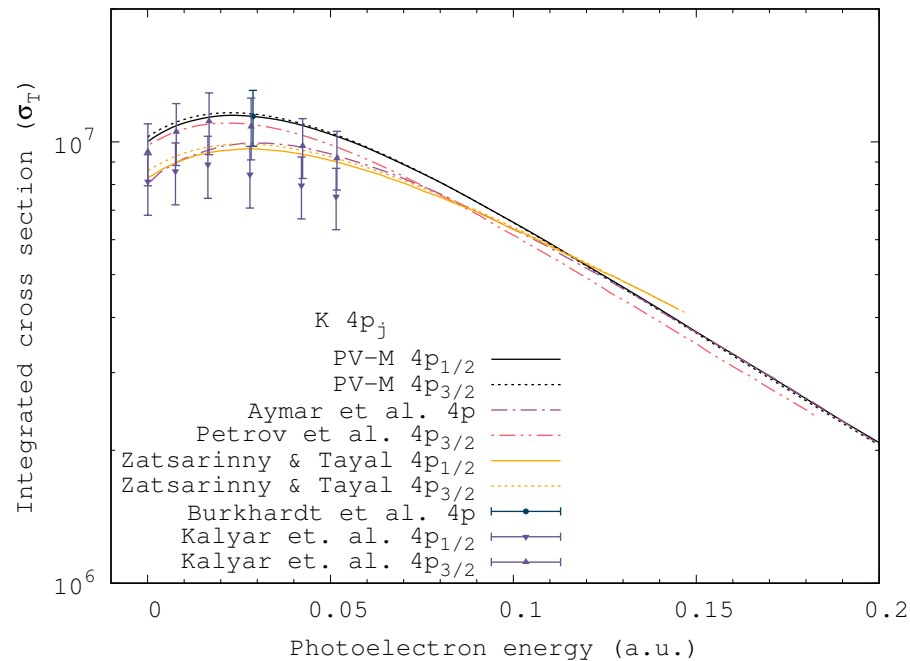
Figure 4. Photoionization cross sections for the $4p_{1/2}$ and $4p_{3/2}$ excited states of potassium calculated using the modified dipole operator. The experimental results of Burkhardt et al. [18] and Kalyar et al. [22] and the theoretical results of Aymar et al. [26], Petrov et al. [28] and Zatsarinny and Tayal [30] are presented for comparison. The results of Amin et al. [20] were virtually identical to those of Kalyar et al. at the corresponding photoelectron energy and were therefore excluded for clarity.

For photoionization from the ground state of potassium, we also compared with the experiments of Hudson and Carter [14], Marr and Creek [15], and Sandner et al. [16] and the calculations of Weisheit [24] and Petrov et al. [29]. We found excellent agreement with the results of Hudson and Carter. We found good agreement with the experiment of Sandner et al. at the Cooper minimum and at lower energies. Our agreement with Marr and Creek and Petrov et al. in the vicinity of the Cooper minimum is poor; however, we found good agreement at higher energies. The potassium photoionization cross section of Weisheit differs from ours at almost all energies, though this difference is small. For photoionization from the $7s_{1/2}$ state of potassium, we found complete agreement with Yar et al. [21] near threshold and the Cooper minimum; at higher energies, our agreement is satisfactory. We found a significant difference between our photoionization cross sections for the $5d_{3/2}$ and $5d_{5/2}$ states and those of Amin et al. [20]. Our $4p_{3/2}$ photoionization cross section is in satisfactory agreement with the experimental values of Kalyar et al. [22], Burkhardt et al. [18], and Amin et al. [20]. Good agreement with the results of Petrov et al. [28] was obtained near threshold; agreement at higher photoelectron energies is not as good. However, our $4p_{1/2}$ cross section is in poor agreement with available theoretical and experimental data. We found that our $4p_{1/2}$ and $4p_{3/2}$ cross sections differed only slightly; Zatsarinny and Tayal similarly only found a small difference between their $4p_{1/2}$ and $4p_{3/2}$ cross sections. The experimental results of Kalyar et al. and Amin et al. suggest a larger difference between these cross sections is expected than what has been predicted in theory.

Having demonstrated that photoionization cross sections for potassium are in excellent agreement with the results of Zatsarinny and Tayal, we now present a comprehensive set of cross sections for lithium, sodium, rubidium, and cesium.

In Figure 5, we present photoionization cross sections for the ground and excited states of lithium. Excellent agreement is found between our results and the calculations of Caves and Dalgarno [23] for photoionization from the ground and excited states of lithium. We compare our ground state photoionization cross sections with the experimental results of Hudson and Carter [13] and Marr and Creek [15] and found poor agreement at all

energies. This is not unexpected as both of these experiments acknowledge that their measurements contain contributions from molecular absorption which must be accounted for. Both experiments account for contributions from alkali metal dimers using a method that relies on vapour pressure data; however, it is difficult to determine how accurate such an approach is due to large uncertainties in the vapour pressure data [16,19].
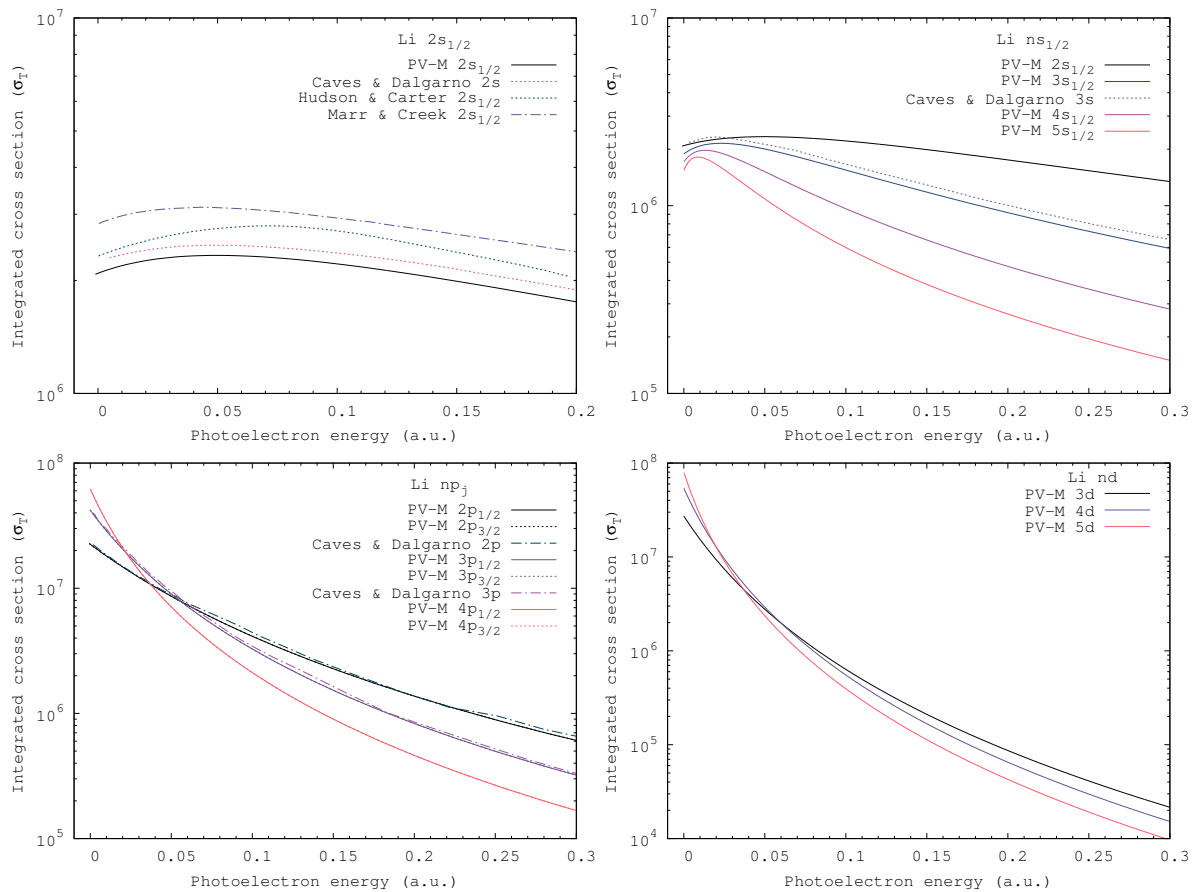

Figure 5. Photoionization cross sections for the ground and excited states of lithium calculated using the modified dipole operator. We compare our ground and excited state photoionization cross section with the experiments of Hudson and Carter [13] and Marr and Creek [15] and the calculations of Caves and Dalgarno [23].

Photoionization cross sections for the ground and various excited states of sodium are presented in Figure 6. Experimental data for ground state photoionization from Hudson [12] and Marr and Creek [15] are also presented for comparison; again, we found poor agreement. We also compared our ground state photoionization cross section with the theoretical results of Weisheit [24] and Petrov et al. [29], and found good agreement with Petrov et al. but not Weisheit. For photoionization from the $3p$ excited states, we found good agreement with the experimental data of Burkhardt et al. [18] and the calculations of Aymar et al. [26] and Petrov et al. [28].

In Figure 7, we present photoionization cross sections for the ground and excited states of rubidium with comparison to the experiments of Marr and Creek [15], Suemitsu and Samson [17] and Lowell et al. [19] and the calculations of Weisheit [24] and Petrov et al. [28,29]. The relative photoionization cross sections of Suemitsu and Samson have been scaled to our results. For photoionization from the ground state, we found poor agreement with available data for both the depth and energy of the Cooper minimum. Our ground state cross section is also smaller than all other results at higher energies. We did, however, find good agreement with the near threshold measurements of Marr and Creek. For photoionization from the $5p_{3/2}$ state, we found good agreement with the calculated cross sections of

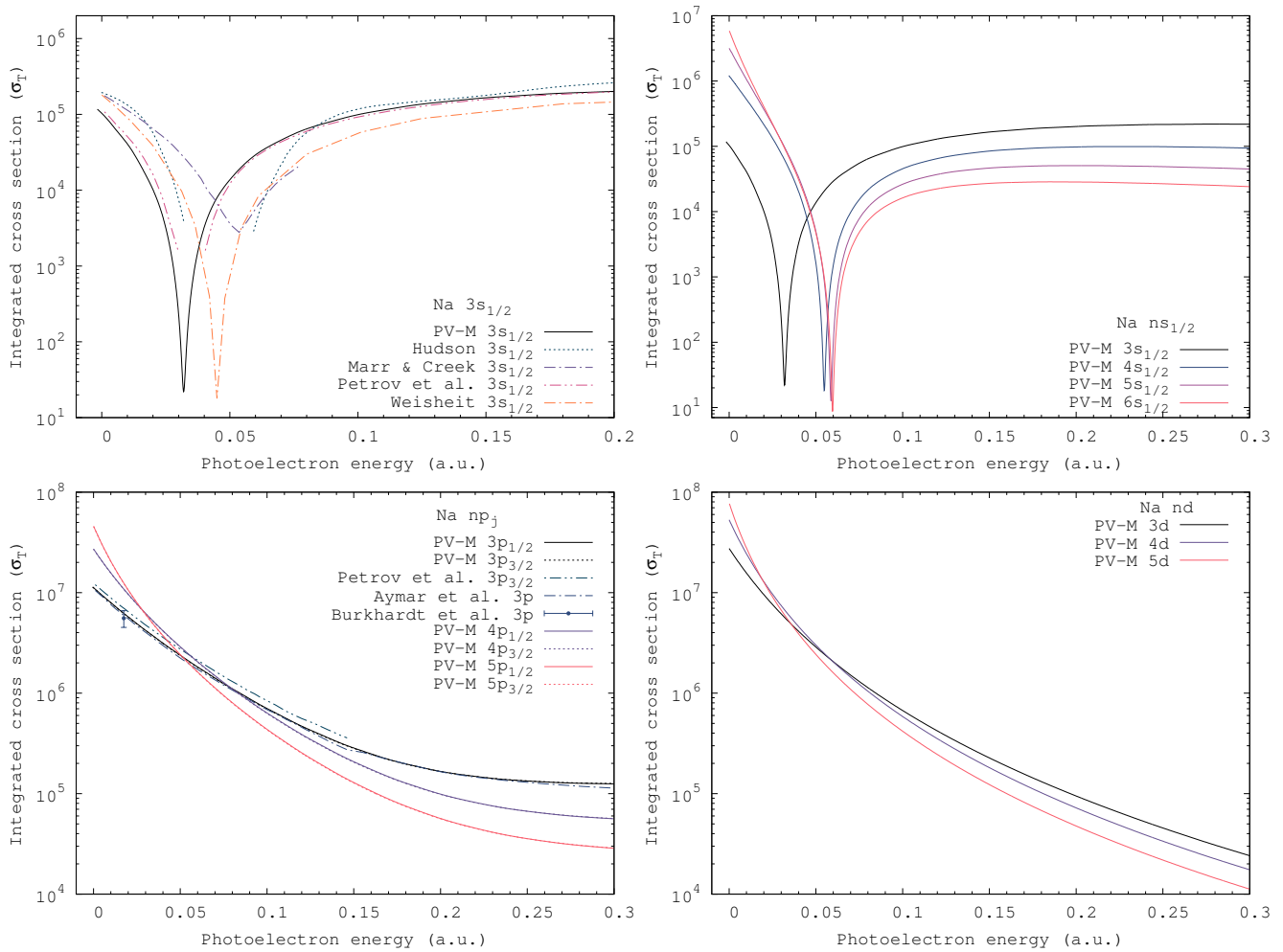Petrov et al. near the ionization threshold, though agreement at higher energies is not as good.

Figure 6. Photoionization cross sections for the ground and excited states of sodium calculated using the modified dipole operator. We compare our photoionization cross sections with the experimental results of Hudson [12], Marr and Creek [15], and Burkhardt et al. [18] and the theoretical calculations of Weisheit [24], Petrov et al. [28,29] and Aymar et al. [26].

Photoionization cross sections from the ground and excited states of cesium are presented in Figure 8 with comparison to the calculations of Weisheit [24], Norcross [25] and Petrov et al. [28,29] and the experiments of Marr and Creek [15] and Suemitsu and Samson [17]. The relative cross sections of Suemitsu and Samson are scaled to our results near the threshold. We found poor agreement with available theoretical data for photoionization from the ground state. Good agreement with the experiment of Suemitsu and Samson was obtained below the Cooper minimum; however, the experiment measured a Cooper minimum that is much narrower than what is predicted by any of the presented theoretical calculations. At higher energies, we found satisfactory agreement with the results of Weisheit. For photoionization from the $6p_{3/2}$ state of cesium, we found good agreement with the near threshold cross section of Petrov et al. However, at higher energies, the agreement is only satisfactory.

The generally poor agreement with available theoretical results for photoionization of rubidium and cesium is not particularly surprising as these atoms are significantly influenced by relativistic effects. This again emphasises the importance of accounting for relativistic effects as well as core polarization.
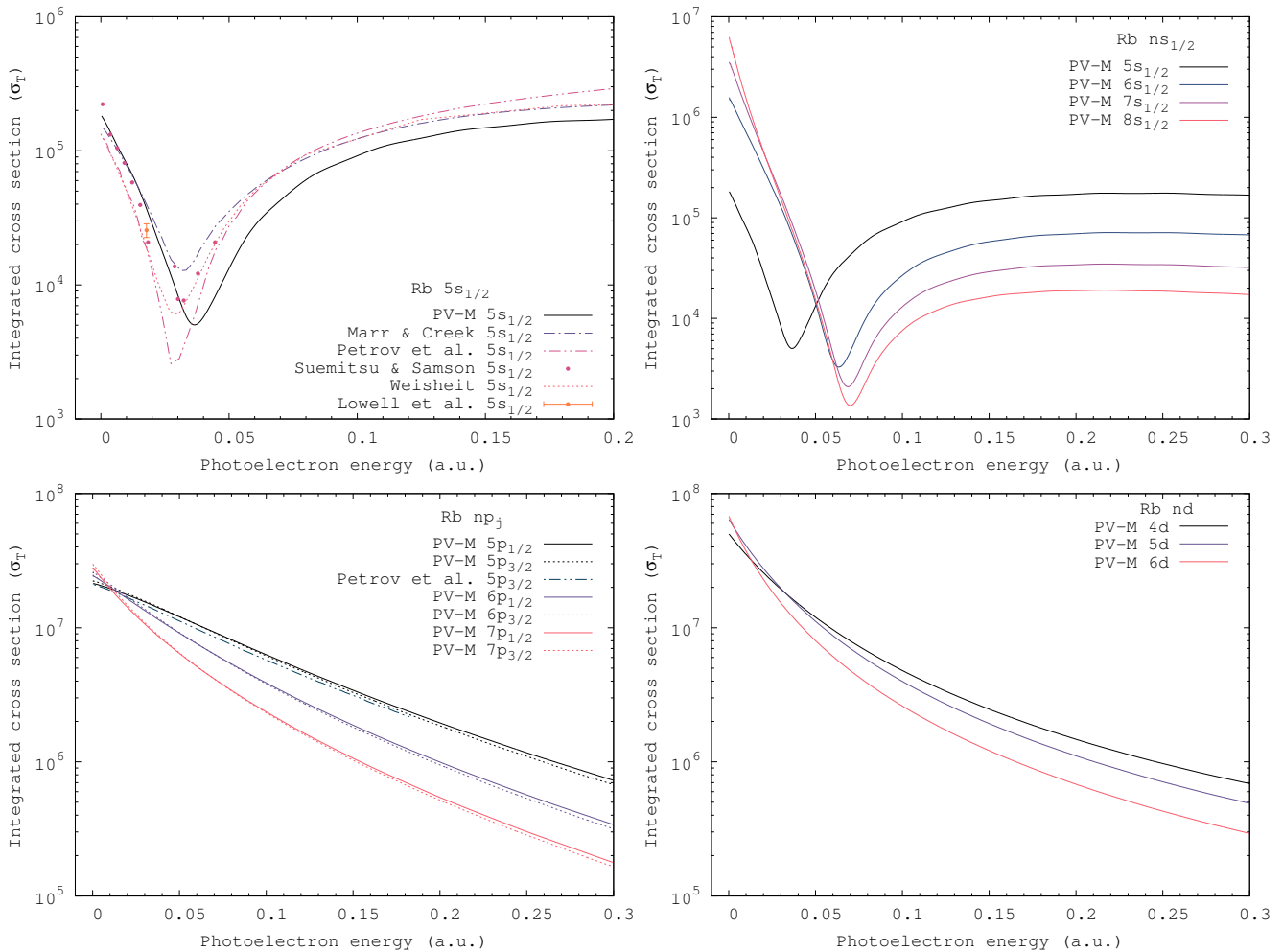

Figure 7. Photoionization cross sections for the ground and excited states of rubidium calculated using the modified dipole operator. Our photoionization cross sections are compared with the experimental results of Marr and Creek [15], Suemitsu and Samson [17], and Lowell et al. [19] and the theoretical calculations of Weisheit [24] and Petrov et al. [29].
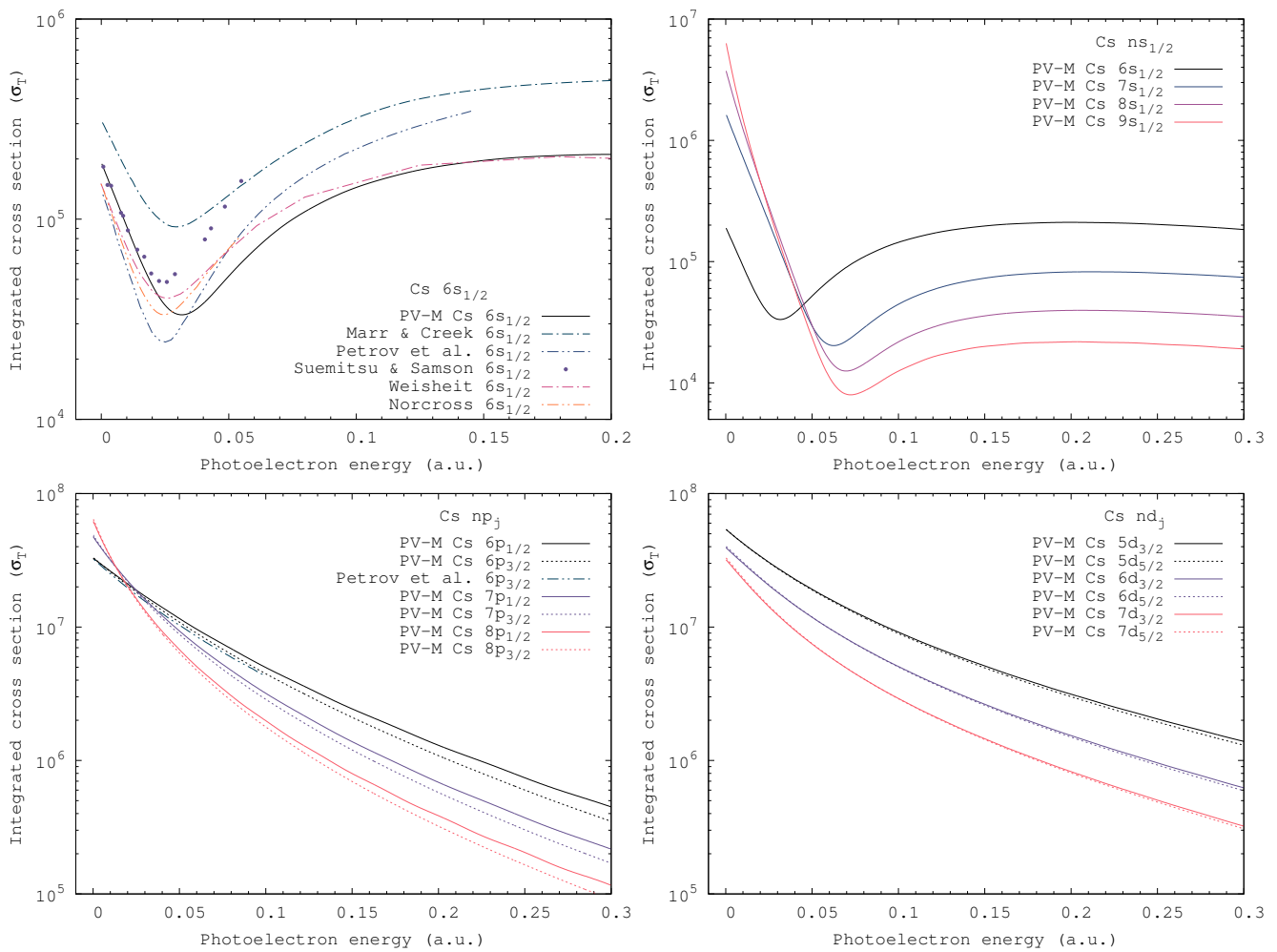
Figure 8. Photoionization cross sections for the ground and excited states of cesium calculated using the modified dipole operator. Our photoionization cross sections are compared with the experimental results of Marr and Creek [15] and Suemitsu and Samson [17] and the theoretical calculations of Weisheit [24], Norcross [25], and Petrov et al. [29].

5. Conclusions

We have presented a fully relativistic method for calculating photoionization using Rayleigh and Raman scattering cross section on quasi one-electron atoms. The method involves a Cauchy principal value integral over the continuum for incident photon energies above the ionization threshold, which results in the necessary components for determining photoionization cross sections being generated automatically whenever Rayleigh scattering cross sections are calculated. We demonstrate the importance of including relativistic effects when calculating photoionization cross sections and Rayleigh and Raman scattering cross sections for incident photon energies above the ionization threshold. We verified our results against the most accurate available theoretical method, the Dirac-based *B*-spline *R*-matrix calculations of Zatsarinny and Tayal [30] for potassium, and found very good agreement. Therefore, we have shown that a model potential method can produce accurate results if both relativistic effects and core polarization are adequately taken into account. Our method was then applied to all other alkali atoms, from lithium to cesium. An extensive set of photoionization cross sections are presented and compared to available experimental and theoretical data. In general, we found good agreement with the experimental results of Sandner et al. [16], Yar et al. [21], and theoretical results of Zatsarinny and Tayal [30] for potassium. New and accurate measurements for the other alkali atoms are highly desirable

to verify present results as the agreement with older experiments and theoretical results is poor.

Author Contributions: Conceptualization, A.S., D.F. and I.B.; methodology, A.S., D.F. and R.M.; software, A.S. and D.F.; validation, A.S. and D.F.; formal analysis, A.S.; investigation, A.S.; resources, D.F. and I.B.; data curation, A.S. and R.M.; writing—original draft preparation, A.S.; writing—review and editing, A.S., D.F., I.B. and R.M.; visualization, A.S.; supervision, D.F.; project administration, D.F. and I.B.; funding acquisition, D.F. and I.B. All authors have read and agreed to the published version of the manuscript.

Institutional Review Board Statement: Not applicable.

Informed Consent Statement: Not applicable.

Data Availability Statement: Available upon request.

Conflicts of Interest: The authors declare no conflict of interest.

Abbreviations

The following abbreviations are used in this manuscript:

KHW	Kramers–Heisenberg–Waller
PV	Principal value

References

1. Kramers, H.A.; Heisenberg, W. Über die Streuung von Strahlung durch Atome. *Z. Phys.* **1925**, *31*, 681–708. [CrossRef]
2. Waller, I. Die Streuung kurzwelliger Strahlung durch Atome nach der Diracschen Strahlungstheorie. *Z. Phys.* **1929**, *58*, 75–94. [CrossRef]
3. Sampson, D.H. The Opacity at High Temperatures due to Compton Scattering. *Astrophys. J.* **1959**, *129*, 734. [CrossRef]
4. Huebner, W.F.; Barfield, W.D. *Opacity*; Springer: New York, NY, USA, 2014.
5. Colgan, J.; Kilcrease, D.P.; Magee, N.H.; Sherrill, M.E.; Abdallah, J., Jr.; Hakel, P.; Fontes, C.J.; Guzik, J.A.; Mussack, K.A. A new generation of los alamos opacity tables. *Astrophys. J.* **2016**, *817*, 116. [CrossRef]
6. Ferraro, J.H.; Nakamoto, K.; Brown, C.W. *Introductory Raman Spectroscopy*; Academic Press: Cambridge, MA, USA, 2003.
7. Lloyd, S. Enhanced Sensitivity of Photodetection via Quantum Illumination. *Science* **2008**, *321*, 1463–1465. [CrossRef] [PubMed]
8. Lanzagota, M. *Quantum Radar*; Morgan & Claypool: San Rafael, CA, USA, 2012.
9. Seaton, M.J. A Comparison of Theory and Experiment for Photo-Ionization Cross-Sections. II. Sodium and the Alkali Metals. *Proc. R. Soc. Lond. Ser. A* **1951**, *208*, 418–430.
10. Fermi, E. Über das Intensitätsverhältnis der Dublettkomponenten der Alkalien. *Z. Phys.* **1930**, *59*, 680–686. [CrossRef]
11. Cooper, J.W. Photoionization from Outer Atomic Subshells. A Model Study. *Phys. Rev.* **1962**, *128*, 681–693. [CrossRef]
12. Hudson, R.D. Atomic Absorption Cross Section of Sodium Vapor Between 2400 and 1000 Å. *Phys. Rev.* **1964**, *135*, A1212–A1217. [CrossRef]
13. Hudson, R.D.; Carter, V.L. Atomic Absorption Cross Section of Lithium Vapor Between 2300 and 1150 Å. *Phys. Rev.* **1965**, *137*, A1648–A1650. [CrossRef]
14. Hudson, R.D.; Carter, V.L. Absorption of Light by Potassium Vapor between 2856 and 1150 Å. *Phys. Rev.* **1965**, *139*, A1426–A1428. [CrossRef]
15. Marr, G.V.; Creek, D.M. The Photoionization Absorption Continua for Alkali Metal Vapours. *Proc. R. Soc. Lond. Ser. A* **1968**, *304*, 233–244.
16. Sandner, W.; Gallagher, T.F.; Safinya, K.A.; Gounand , F. Photoionization of potassium in the vicinity of the minimum in the cross section. *Phys. Rev. A* **1981**, *23*, 2732–2735. [CrossRef]
17. Suemitsu, H.; Samson, J.A.R. Relative photoionization cross sections of Cs, Cs_2, Rb, and Rb_2. *Phys. Rev. A* **1983**, *28*, 2752–2758. [CrossRef]
18. Burkhardt, C.E.; Libbert, J.L.; Xu, J.; Leventhal, J.J.; Kelley, J.D. Absolute measurement of photoionization cross sections of excited atoms: Application to determination of atomic beam densities. *Phys. Rev. A* **1988**, *38*, 5949–5952. [CrossRef] [PubMed]

19.   Lowell, J.R.; Northup, T.; Patterson, B.M.; Takekoshi, T.; Knize, R.J. Measurement of the photoionization cross section of the $5S_{1/2}$ state of rubidium. *Phys. Rev. A* **2002**, *66*, 062704. [CrossRef]

20.   Amin, N.; Mahmood, S.; Haq, S.U.; Kalyar, M.A.; Rafiq, M.; Baig, M.A. Measurements of photoionization cross sections from the 4p, 5d and 7s excited states of potassium. *J. Quant. Spectrosc. Radiat. Transf.* **2008**, *109*, 863–872. [CrossRef]

21.   Yar, A.; Ali, R.; Baig, M.A. Evidence of a Cooper minimum in the photoionization from the $7s\,^2S_{1/2}$ excited state of potassium. *Phys. Rev. A* **2013**, *88*, 033405. [CrossRef]

22.   Kalyar, M.; Yar, A.; Iqbal, J.; Ali, R.; Baig, M. Measurements of photoionization cross section of the 4p levels and oscillator strength of the 4p→nd 2D3/2,5/2 transitions of potassium. *Opt. Laser Technol.* **2016**, *77*, 72–79. [CrossRef]

23.   Caves, T.; Dalgarno, A. Model potential calculations of lithium transitions. *J. Quant. Spectrosc. Radiat. Transf.* **1972**, *12*, 1539–1552. [CrossRef]

24.   Weisheit, J.C. Photoabsorption by Ground-State Alkali-Metal Atoms. *Phys. Rev. A* **1972**, *5*, 1621–1630. [CrossRef]

25.   Norcross, D.W. Photoabsorption by Cesium. *Phys. Rev. A* **1973**, *7*, 606–616. [CrossRef]

26.   Aymar, M.; Luc-Koenig, E.; Farnoux, F.C. Theoretical investigation on photoionization from Rydberg states of lithium, sodium and potassium. *J. Phys. B At. Mol. Phys.* **1976**, *9*, 1279–1291. [CrossRef]

27.   Saha, H.P. Numerical multiconfiguration self-consistent-field studies of atomic photoionization cross sections: Dynamical core-polarization effects in atomic potassium. *Phys. Rev. A* **1989**, *39*, 628–633. [CrossRef]

28.   Petrov, I.D.; Sukhorukov, V.L.; Leber, E.; Hotop, H. Near threshold photoionization of excited alkali atoms Ak(np) (Ak = Na, K, Rb, Cs; n = 3–6). *Eur. Phys. J. D* **2000**, *10*, 53–65. [CrossRef]

29.   Petrov, I.D.; Sukhorukov, V.L.; Hotop, H. The influence of core polarization on photo-ionization of alkali and metastable rare gas atoms near threshold. *J. Phys. B At. Mol. Opt. Phys.* **1999**, *32*, 973–986. [CrossRef]

30.   Zatsarinny, O.; Tayal, S.S. Photoionization of potassium atoms from the ground and excited states. *Phys. Rev. A* **2010**, *81*, 043423. [CrossRef]

31.   McNamara, K.; Fursa, D.V.; Bray, I. Efficient calculation of Rayleigh and Raman scattering. *Phys. Rev. A* **2018**, *98*, 043435. [CrossRef]

32.   Singor, A.; Fursa, D.; McNamara, K.; Bray, I. Rayleigh and Raman Scattering from Alkali Atoms. *Atoms* **2020**, *8*, 57. [CrossRef]

33.   Balslev, E.; Combes, J.M. Spectral properties of many-body Schrödinger operators with dilatation-analytic interactions. *Commun. Math. Phys.* **1971**, *22*, 280–294. [CrossRef]

34.   Simon, B. Quadratic form techniques and the Balslev-Combes theorem. *Commun. Math. Phys.* **1972**, *27*, 1–9. [CrossRef]

35.   Rescigno, T.N.; McKoy, V. Rigorous method for computing photoabsorption cross sections from a basis-set expansion. *Phys. Rev. A* **1975**, *12*, 522–525. [CrossRef]

36.   Sakurai, J. *Advanced Quantum Mechanics*; Addison-Wesley: Reading, MA, USA, 1967.

37.   Babushkin, F.A. A Relativistic Treatment of Radiation Transitions. *Opt. Spectrosc.* **1962**, *13*, 77.

38.   Babushkin, F.A. Relativistic Radiation Transitions. *Opt. Spectrosc.* **1965**, *19*, 1–2.

39.   Grant, I.P. Gauge invariance and relativistic radiative transitions. *J. Phys. B At. Mol. Phys.* **1974**, *7*, 1458–1475. [CrossRef]

40.   Sobelman, I. *Atomic Spectra and Radiative Transitions*; Springer Series in Chemical Physics; Springer: Berlin/Heidelberg, Germany, 1979.

41.   Dyall, K.; Grant, I.; Johnson, C.; Parpia, F.; Plummer, E. GRASP: A general-purpose relativistic atomic structure program. *Comput. Phys. Commun.* **1989**, *55*, 425–456. [CrossRef]

42.   Furness, J.B.; McCarthy, I.E. Semiphenomenological optical model for electron scattering on atoms. *J. Phys. B At. Mol. Phys.* **1973**, *6*, 2280–2291. [CrossRef]

43.   Albright, B.J.; Bartschat, K.; Flicek, P.R. Core potentials for quasi-one-electron systems. *J. Phys. B At. Mol. Opt. Phys.* **1993**, *26*, 337–344. [CrossRef]

44.   Mitroy, J.; Griffin, D.C.; Norcross, D.W.; Pindzola, M.S. Electron-impact excitation of the resonance transition in Ca^+. *Phys. Rev. A* **1988**, *38*, 3339–3350. [CrossRef] [PubMed]

45.   Hameed, S.; Herzenberg, A.; James, M.G. Core polarization corrections to oscillator strengths in the alkali atoms. *J. Phys. B At. Mol. Phys.* **1968**, *1*, 822–830. [CrossRef]

46.   Cheng, Y.-S.; Liu, J.-C.; Sun, W.-G. Core polarization corrections for the photoionization of sodium. *Acta Phys. Sin. (Overseas Ed.)* **1998**, *7*, 161–166.

47.   McEachran, R.P.; Ryman, A.G.; Stauffer, A.D.; Morgan, D.L. Positron scattering from noble gases. *J. Phys. B At. Mol. Phys.* **1977**, *10*, 663–677. [CrossRef]

48.   Lim, I.S.; Laerdahl, J.K.; Schwerdtfeger, P. Fully relativistic coupled-cluster static dipole polarizabilities of the positively charged alkali ions from Li+ to 119+. *J. Chem. Phys.* **2002**, *116*, 172–178. [CrossRef]

49.   Sternheimer, R.M. Quadrupole Polarizabilities of Various Ions and the Alkali Atoms. *Phys. Rev. A* **1970**, *1*, 321–327. [CrossRef]

50.   Grant, I.P.; Quiney, H.M. Rayleigh-Ritz approximation of the Dirac operator in atomic and molecular physics. *Phys. Rev. A* **2000**, *62*, 022508. [CrossRef]

51.   Bostock, C.J. The fully relativistic implementation of the convergent close-coupling method. *J. Phys. B At. Mol. Opt. Phys.* **2011**, *44*, 083001. [CrossRef]

52.   Sienkiewicz, J.E.; Baylis, W.E. A relativistic approach to the elastic scattering of electrons by argon. *J. Phys. B At. Mol. Phys.* **1987**, *20*, 5145–5156. [CrossRef]

53. Fursa, D.V.; Bray, I. Fully Relativistic Convergent Close-Coupling Method for Excitation and Ionization Processes in Electron Collisions with Atoms and Ions. *Phys. Rev. Lett.* **2008**, *100*, 113201. [CrossRef]
54. Fursa, D.V.; Bostock, C.J.; Bray, I. Relativistic convergent close-coupling method: Calculations of electron scattering from cesium. *Phys. Rev. A* **2009**, *80*, 022717. [CrossRef]